Estimation of long term spatiotemporal patterns of land surface temperature in response to land use land cover (LULC) change and formation of urban heat island for Lahore city, Pakistan

By

Mohsin Ramzan

(Reg. No 00000172291)

A thesis submitted in partial fulfillment of the requirements for the degree of Master of Science in Remote Sensing and GIS

Institute of Geographical Information Systems
School of Civil and Environmental Engineering
National University of Sciences & Technology
Islamabad, Pakistan

July, 2019

THESIS ACCEPTANCE CERTIFICATE

Certified that final copy of MS/MPhil thesis written by Mr. Mohsin Ramzan, (Registration No. 00000172291), of IGIS-SCEE-NUST has been vetted by undersigned, found complete in all respects as per NUST statutes/Regulations, is free of plagiarism, errors and mistakes and is accepted as partial fulfillment for award of MS/MPhil degree. It is further certified that necessary amendments as pointed out by GEC members of the scholar have also been incorporated in the said thesis.

Signature: _____

Name of Supervisor: Dr. Ejaz Hussain

Date: _____

Signature (HOD): _____

Date: _____

Signature(Dean/Principal): _____

Date: _____

ACADEMIC THESIS: DECLARATION OF AUTHORSHIP

I, Mohsin Ramzan, declare that this thesis and the work presented in it are my own and have been generated by me as the result of my own original research work.

Estimation of long term spatiotemporal patterns of land surface temperature in response to land use land cover (LULC) change and formation of urban heat island using Landsat data of Lahore city, Pakistan

I confirm that;

1. This thesis is composed of my original work, and contains no material previously published or written by another person except where the references have been made in the text ;
2. Wherever any part of this thesis has previously been submitted for a degree or any other qualification at this or any other institution, it has been clearly stated;
3. I have acknowledged all main sources of help;
4. Where the thesis is based on work done by myself jointly with others, I have made clear exactly what was done by other and what I have contributed myself;
5. None of this work has been published before submission;
6. This work is not plagiarized under HEC plagiarism policy.

Signed: _____

Date: _____

DEDICATION

"To my loving mother (late) for making me who I am,

And,

My father for supporting me all the way…"

ACKNOWLEDGEMENTS

After thanking Almighty Allah Almighty who is the only source of knowledge and to the Holy Prophet Muhammad (Peace and blessings be upon Him) who passed His knowledge to humanity, as a whole, I would like to thank my parents for their constant support and motivation.

I convey my sincere gratitude to my supervisor prof. Dr. Ejaz Hussain (IGIS, NUST) for rendering his valuable time, supervision, and assistance for the improvement of this dissertation. I extend my regards and unreserved gratitude to my committee members; Prof. Dr. Javed Iqbal (IGIS), Dr. Abdul Waheed (NIT) and Mr. Junaid Aziz Khan (IGIS) for rendering their valuable time, beneficial guidance, kind words of encouragement and cooperation throughout the entire course of research work.

I am also highly grateful to Pakistan Meteorological department for providing me the relevant data without any hesitation. I am sincerely obliged to NUST and IGIS to have provided me the adequate research fund for the completion of this research work.

TABLE OFCONTENT

LIST OF FIGURES

LIST OF TABLES

ABSTRACT

An urban heat island (UHI) is a metropolitan area having high temperature surrounded by area with relatively low temperature formed by absorption of heat from sunlight by construction materials. Thermal remote sensing provides a time synchronous temperature data for comparatively a large area. The aim of this research is to estimate land surface temperature (LST) during summer seasons through remotely sensed data and relate it to UHI corresponding to urbanization. Temporal data of Landsat as well as MET data of temperature and precipitation from 1990 to 2017 were used to identify and analyze the UHIs. Different indices such as NDVI, NDBI, and NDBaI were used to detect and map different types of land use land cover's (LULC) attributes for quantitative and qualitative image analysis as changes in LULC causes change in reflectance of land surface. Correlation between different parameters such as LST and Air Temperature, built up land, and Indices were investigated. An overall increase of 41% in built up area, 23%, 17% and 0.4% decrease in the area of vegetation, bare land and water was observed from 1992 to 2017 respectively. Comparison of temperature from MET station and satellite image showed an increasing trend in LST (29.5°C to 33.6°C from 1992-2017). The mean LST over different LULCs showed a similar increasing trend but the increase was significant for built up (28.4°C to 35.5°C from 1992-2017) implying the significant effect of urbanization on LST. Based on the existing trend, future trends of LULC and LST were predicted for years 2021, 2025, and 2030 using Markov Model. These changes in LULC and LST in turn have detrimental effects on local as well as global climate, environmental degradation, and water resources. The study will help in understanding and addressing these issues.

Chapter 1

INTRODUCTION

Several physical features of a landscape combine to influence local climate variations, main among these are topography, proximity to water bodies, and urbanization. Urbanization refers to physical growth of an urban area in terms of population and man-made features compared to surrounding rural areas. Human settlements through rapid urbanization are constantly modifying the surface energy balance, structure of earth surface and composition of atmosphere compared to the surrounding 'natural' terrain, hence accounting towards the distinct alteration of land covers and subsequently the land use (Zhang *et al.*, 2009). According to UN Millennium Development Goals Report (2017), half of the world's human population is now residing in cities/ urban areas. It is expected that in future (by 2030), the global rate of urbanization will increase by 70% of the present world urban population due to the continuing and rising trend in rural to urban migration. For this reason, it is not surprising to see the increasing concern scientists are now showing worldwide towards these negative impacts of urbanization (McConnell *et al.*, 2009).

Urban growth is measured through both area and population; the latter being directly proportional to the former, therefore as the city grows, more impervious built-up/urban land develops which drastically changes the surface physical characteristics- the most important one being surface temperature variation. While studying urban climates, land surface temperature (LST) is very important. LST alters the air temperature and stands as a major player in the surface energy balance by efficiently portioning latent heat fluxes

and consequently the temperature radiated by surfaces with varying soil water content and vegetation cover, thus significantly effecting the local weather and climate (Kalnay & Cai, 2003).

The shifting trends in temperature can be clearly witnessed while travelling from urban downtown area to suburban or rural surroundings, and vice versa. This is due to distinct landscapes of both areas; the urban largely comprises of asphalt and concrete material, infrastructure and other paved surfaces, while the rural consists of more natural vegetation cover, pastures and flora etc. This variability in LULC in urban areas causes them to suffer from more solar radiation absorption and increased thermal conductivity (Weng, 2009; Xian & Crane, 2006). One can feel blistering heat waves in hot summers emitting from dark buildings and other infrastructure which make urban areas warmer and keep them hot even long after the sunset, while the rural areas rapidly cools down. This phenomenon of customized climate is known as the Urban Heat Island (UHI) effect, and has been documented for over 150 years (Voogt & Oke, 2003; Xiao & Weng, 2007).

The concept of UHI was first proposed by Manley (1958), who stated that a 'thermal isolated island' is generated when a city expands to such an extent that it changes the properties of its underlying surface and eventually suffers from severe air population, releasing substantial waste heat producing temperature considerably higher as compared to the surrounding rural regime. The U.S. Environmental Protection Agency (EPA) defines the phenomenon of UHI through the same reasoning that '*replacement of vegetation by asphalt and concrete surfaces such as buildings, roads, etc. in order to accommodate growing population gives birth to formation of heat islands. These surfaces absorb more heat from the sun resulting in an increased surface temperature* (Ward *et*

al., 2016). UHI effects are further aggravated by the anthropogenic heat generated through industrial activities, vehicular traffic and other human activities in busy commercial areas (Dousset & Gourmelon, 2003; Streets *et al.*, 2009; Yuan & Bauer, 2007). Of all the reasons mentioned above, the most significant contributor of UHI effect is the difference in the thermal characteristics of the surface areas as a result of the constantly changing LULC types in urban area (Streets *et al.*, 2009).

Heat islands are formed both at surface and in the atmosphere, while surface UHI's are usually present both at day and night but these are stronger in the day time when sun is shining. Atmospheric UHI's are weak in the day time and become stronger after sunset due to slow emission of heat from the urban infrastructure. (Figure 1.1). Hence, nature of land cover type can affect the surface temperature (US EPA, 2014). The enormity of surface UHIs varies with the seasons, resulting from change in intensity of solar radiation along with the ground cover and climatic conditions. Therefore, UHIs are typically more prominent in the summer (Tomlinson *et al.*, 2012; Xiao & Weng, 2007).

UHIs results in increased energy demand and consequently the energy costs and quality of urban life. The rate of change of energy consumption is reportedly twice the rate of change in urbanization. Increased urban temperatures directly affect the energy consumption in buildings during summer season, as electricity demand for cooling amplifies the air conditioning and refrigeration, thus producing greenhouse gases and other pollutants which further add to the depletion of ozone and may give way to global warming (Feizizadeh & Blaschke, 2013; Xiong *et al.*, 2012; Zhou *et al.*, 2011). Apart from the apparent effects, UHIs are known to have some other effects on the local weather i.e. the alteration of wind patterns, the formation of clouds, fog and smog, increase in the

number thunderbolt strikes, sudden cloud bursts and rates of precipitation (Barnett *et al.*, 2005; Miao *et al.*, 2011; Xiong *et al.*, 2012).

Traditional studies on UHI were profoundly conducted by the collecting ground based observation of temperature observed from network of fix weather observatories, or by thermometer carrying moving vehicles(Weng *et al.*, 2019). These techniques proved extremely time consuming and tough when detailed spatial distribution of temperature is required. Remote sensing has effectively made up for this tribulation with the advantages of synoptic coverage and temporal repetition offered by multiple satellite and aircraft platforms. Surface temperature patterns and that of other thermal energy environments can now be acquired extensively and effortlessly by using thermal sensor data in the study of the urban climates(Weng *et al.*, 2019). Further incorporating the Geographic Information Systems (GIS) along with the RS technology, the ability to retrieve, monitor, analyze, manipulate and interpret the geospatial data is greatly enhanced.

1.1 STUDY AREA

Lahore is one of the largest districts of Pakistan in terms of population of about 11.2 million (Census 2017) which was 6.3 million in 1998. It is also one of the largest cities of Punjab in terms of area and is also the commercial capital of the country. It is geographically situated on latitude 31°15′ to 31°45′ N and longitude of 74°01′ to 74°39′ E respectively, and has an area of 1,772 km². Its population has increased so rapidly that it has almost been doubled in 20 years. It has been selected as study area because the effect of urbanization in the long run on LST has not yet been measured on local scale and it is frequently changing with in terms of LULC because of the quick change in population due to rapid economic growth. It exhibits rapid environmental changes in

terms of air temperature and perviousness to imperviousness ratio because of high rate of urbanization in the city resulting in heat trap and causing a rise in temperature. It has relatively modern infrastructure though at the cost of environmental sustainability. Inadequate infrastructure has led to an increase in traffic congestion in city. Because of High urbanization most of the land cover is impervious in nature, which leads to a several urban environmental issues such as increase in runoff generation and LST etc. Most of the land cover in the city is industrial in nature which is spreading alarmingly and encroaching into adjacent non-urban land. Moreover, lack of sufficient urban facilities, especially sewerage and drainage conditions, and solid waste management, have further aggravated the quality of life and environmental conditions. This indicates the potentiality of this area to carry a research on LST and its suitability for UHI analysis.

The study area map is given in Figure 1.2.

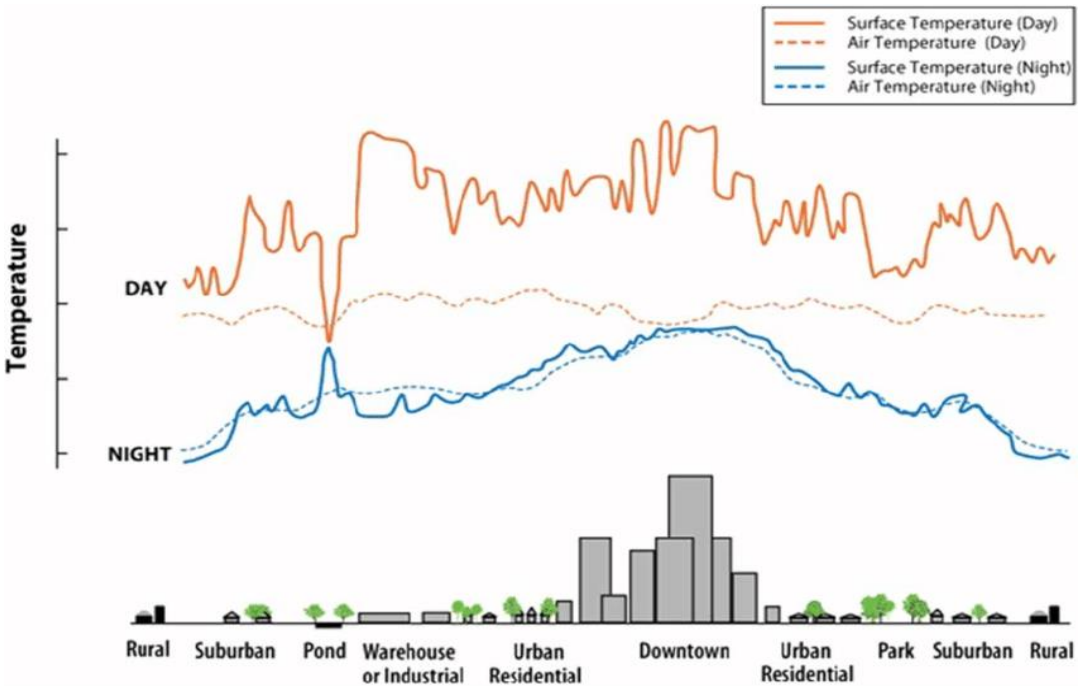

Figure 1.1: Typical Urban Heat Island Profile (Source: US EPA. 2009)

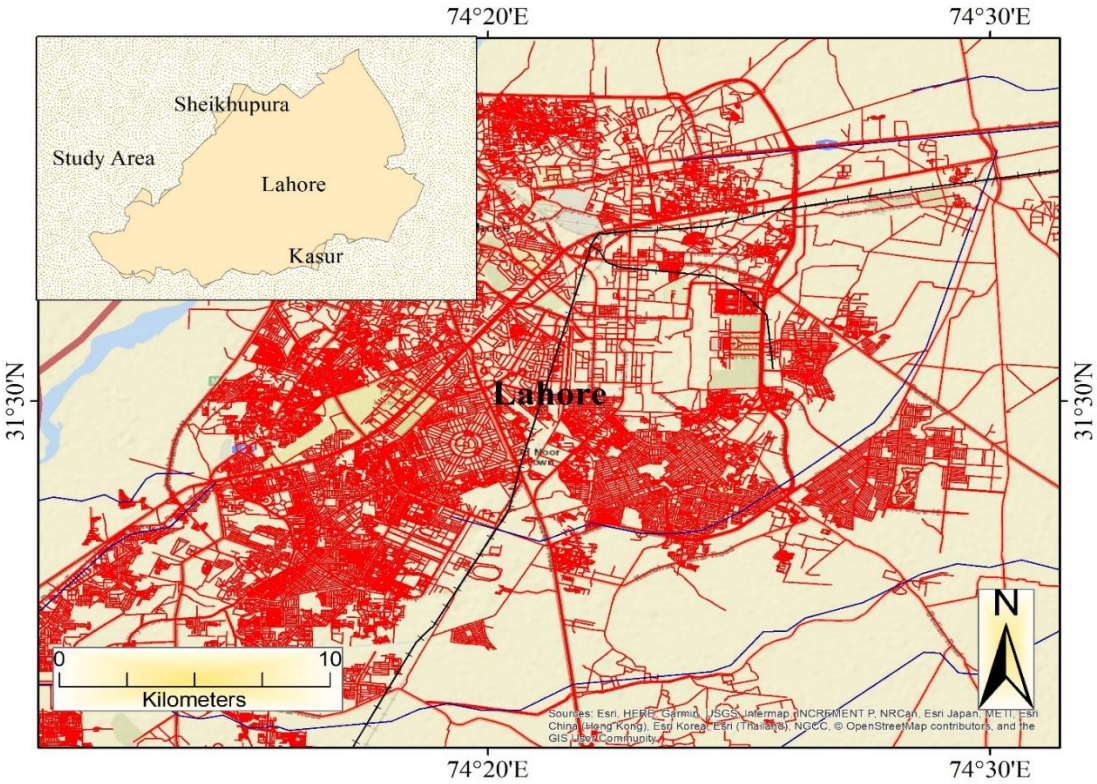

Figure 1.2: Study Area

1.2 SIGNIFICANCE

Urbanization is one of the major concerns among social scientists and other planning authorities in the developing world. Changes in LULC pattern in relation to urban growth have made city environments congested, mainly because of inappropriate planning. This noticeably impacts the local temperature of an area, therefore creating heat islands that are now abundantly prevalent in almost all densely populated cities around the globe. Recently these haphazardly imposed LULC changes have become the focal point of all the present researches pertaining to rising environmental and socio-economic issues in urban areas (Streets *et al.*, 2009). Studies of temporal analysis depicting LULC changes in a region greatly help in explaining the spatial extent and the degree of the change itself, through assessment of direction and degree of these human-induced transformations (Li *et al.*, 2016; Xiao & Weng, 2007).

UHIs tend to have a direct influence on health and wellbeing of urban dwellers. Increase in temperature results in rise of degree and extent of heat waves in urban areas. It has been proven in a Research that mortality rate increases exponentially with the temperature when a heat wave occurs (Patz *et al.*, 2005).

Extensive studies have made use of the GIS and RS technology to address the UHI effect; the most being done in developed countries like Europe and North America. But countries like China, Japan, Singapore, India and Israel have not been far behind, as most of their respective researches are sprouting with this grave issues concerned with urban climates. This study is an attempt for investigating the UHI effect in one of the most important areas of Pakistan i.e. the Lahore district through the analysis of its urban land cover changes over the past two decades. By determining the existing spatial processes of urban

growth in the city, the intensity of the resulting UHI effect and temperature variations are also brought about. This would help in bringing forward the urgent need and importance of proper land use planning and controlled energy consumption, this giving weight to the development and protection of green areas in the region for a cooler environment.

1.3 SCOPE OF STUDY

The primary purpose of this study is to quantitatively estimate UHI effect from various RS data for the period from 1992-2017 and correlate it with the changes in LULC in the Lahore city due to rapid urbanization in the region. For this purpose Landsat TM5 and Landsat 8 OLI/TIRS imageries have been used for the retrieval of LST and LULC types in order to examine the changes in LULC types during the summer months of May or June (depending upon the availability of data to minimize the variation among land surface cover and atmospheric effects), spanning over a period of 1992 to 2017 respectively.

Detailed image analysis were conducted in order to monitor the impact of LULC changes on the spatial distribution of LST, thus evaluating the UHI effect. Multiple indices such as NDVI, NDBI, and NDBaI were used to extract LULC information and subsequently were quantitatively analyzed with the LST calculated from the thermal (TIR) band, along with the ambient air temperature from weather stations. The impact of LULC changes on the surface temperature was also assessed by predicting the future contribution of LST of each LULC type towards the overall temperature of the study area, from the present and past data through a quantitative scenario building process.

This thesis contains six chapters and supporting references. In chapter 1, background material that was needed to fully understand the importance of the research is discussed.

Chapter 2 reviews the critical points and gives a comprehensive survey of related research work, while chapter 3 gives detailed description of the data used and its processing along with the research methodology, and GIS analysis conducted on the data. The results of GIS analysis are discussed in chapter 5 followed by conclusions, and recommendation in chapter 6 respectively.

1.4 OBJECTIVES & HYPOTHESIS

The overall objective of the research is to evaluate the relationship between UHI effect and LULC changes in study area by making efficient use of the RS and GIS technology. However, the study specifically aims at:

a) Identification and Mapping of temporal LULC changes and estimation of LST (1992-2017)

b) Comparison and analysis of temporal LULC and LST, and identification of UHIs

c) Prediction of LST trends as a result of urbanization

The relationship between LST and LULC change types is formulated by generating a research hypothesis, which is:

“Change in land cover type induces change in urban temperatures, all other factors being constant.”

Chapter 2

LITERATURE REVIEW

The benefit remote sensing and GIS has been providing to its researchers, since its advent and till date, is immense and somewhat immeasurable. As the technology progresses, so does its applications and prospects. Across the globe developed as well as developing nations are striving to make full use of this technology in almost every walk of life. The different disciplines this technology caters to are expanding day by day, from the mapping of disease outbreaks, archeological sites and crime analysis, to the assessment of business and marketing efforts. Almost all environmental issues have been addressed by researchers using GIS and RS, thus greatly broadening our horizons and eventually leading towards a better understanding of the world we are living in and where it is headed.

The UHI effect has long been the hot topic of climatic research (Mitchell, 1961). According to Oke (1973), even a town of 1000 people could experience the UHI effect due to its linear correlation with population(Oke, 1973). Therefore, the use of RS technology for the mapping and measurement of UHIs is apt for macro scale studies.

The complex structure of cities comprises of infrastructures, bio-diversity, and human organizations (Buyantuyev & Wu, 2010; Weng *et al.*, 2014; Weng *et al.*, 2004). Urbanization plays a major role in replacement of vegetation cover with the impervious surfaces such as concrete buildings, asphalt roads, and other paved surfaces (Tayyebi *et al.*, 2018). This type of conversion of land cover has a remarkable effect on local climate in terms of land surface temperature (Change, 2014) and imposes a variety of negative

consequences related to environment as well as human life. Some of the negative consequences include biodiversity loss (Higgins, 2007), water scarcity (Barnett *et al.*, 2005) increased heat-related mortality (Foley *et al.*, 2005; Patz *et al.*, 2005), increased energy demand (Kikegawa *et al.*, 2006), and increased air pollution (Stone Jr, 2005, 2008). Therefore, assessment of effects of urbanization on spatio-temporal variation of LST in longer term becomes vital (Grimmond, 2007).

Moreover, land cover, elevation, and climate conditions participate in formation of urban heat and LST patterns in mega-cities (Fu & Weng, 2016a, 2016b; Li *et al.*, 2016; Zhou *et al.*, 2011) . Urban heat can be reduced by increasing vegetation since it has high evapotranspiration (Tomlinson *et al.*, 2012). The amount and intensity of urban heat varies with time during the day and with the season accordingly (Buyantuyev & Wu, 2010; Yao *et al.*, 2018). The absorption of heat by impervious surfaces during the day and emission at night, change in sun's intensity and solar illumination angle, and the change in ground cover are some of the main causes of variation in urban heat during the day and night, and according to seasons(Maimaitiyiming *et al.*, 2014; Tayyebi *et al.*, 2018). Morris et al. (2001), found that variation in urban heat were higher in summer as compared to winter (Torok *et al.*, 2001).

Urbanization can cause a significant change in local weather and climate. One of the most familiar effect of urbanization is UHI which directly represents the degree of environmental degradation. UHI is any metropolitan area which is relatively warm in temperature than the surrounding rural area. Acceleration in urbanization leads to formation of more distinct UHIs. Impervious surfaces such as tall concrete buildings, asphalt roads, narrow streets, and parking lots etc. traps the heat hence reducing the air

flow between them. Moreover, UHIs are also formed because of presence of industrial activities in urban areas. Replacement of pervious surfaces with impervious surfaces replaces the natural cooling effect. In addition vehicular heat, heat from factories and air conditioners further add warmth to the atmosphere, thus increasing the UHI effects. Thus, there are variations in day, night and seasonal measurements of LST. Landsat TM data is one of the most widely used satellite images for LST retrieving because of free availability of thermal band (120 m for thermal, 30 m for visible and infrared bands). Keeping the above facts in view, the Lahore city has been selected for carrying out the retrieval of LST and estimation of UHIs as it is experiencing very rapid growth in population and urbanization.

Chapter 3

MATERIALS AND METHODS

The Lahore city has undergone major developments and improvements in terms of infrastructure and expansion through the influence of urbanization since 1990s. Keeping in mind the research objectives, relevant materials and methods were selected for the study, the details are given below:

3.1 MATERIALS

In order to quantitatively derive LST and determine LULC type changes for the computation of UHI effect in the study area from 1992 to 2017, two types of sensors data were utilized, namely; Landsat 5 TM and Landsat 8 OLI/TIRS. Landsat 5 provided imageries for the period before 2008 and Landsat 8 for year 2017.

Landsat 5 launched in 1984, has 7 bands. Band 1-5 and 7 have nominal spatial resolution of 30m, while the thermal infrared band (band 6) has 120m spatial resolution.

Landsat 8 launched in February 2013, has two sensors mounted on it one is Operational Land Imager (OLI) and the other is Thermal Infrared Sensor (TIRS). OLI has 9 spectral bands including panchromatic band; all except the panchromatic band have a spatial resolution of 30m whereas the panchromatic has a spatial resolution of 15m. TIRS have two thermal bands and have a spatial resolution of 100m. ArcMap 10.6 and ERDAS Imagine were used for the processing and analysis of the respective satellite imageries.

3.1.1 Satellite Data

Four Landsat 5 TM images (Cloud cover less than 10%) acquired on June 1992, July 1996, May 2000, and June 2008; and two image of Landsat 8 OLI/TIRS (Cloud cover

less than 10%) acquired on June 2014 and June 2017 were used respectively. These imageries were acquired from United States Geological Survey's (USGS) website. These images were atmospherically corrected. Details of the datasets are given in the Table 3.1.

3.1.2 Meteorological Data

Two meteorological parameters, temperature and rainfall were utilized for the research, for which the data were collected from Pakistan Meteorological Department (PMD) Lahore. Apart from the average data for the respective satellite image dates, it was essential to obtain hourly temperature data as each satellite has its own respective image acquisition time. However, hourly temperature data for the PMD station was not available as it is collected at specific times, i.e. 0800, 1400 and 1700 PST. Rainfall data were needed in order to check any precipitation prior to image acquisition which might alter the temperature ranges.

3.2 METHODS

A methodology was developed to analyze the temporal LULC changes and UHI effect in the region (Figure 3.1). The climate data were utilized for relating the ambient air temperature with the near surface temperature derived from the respective imageries. The processed imageries were used for LULC classification, retrieval of vegetation, bare land and built-up indices, and calculation of brightness temperature from radiance in order to finally retrieve the required LST in the study area. Finally the LULC and LST trends were predicted. The schema for methodology adopted is given in (Figure 3.1)

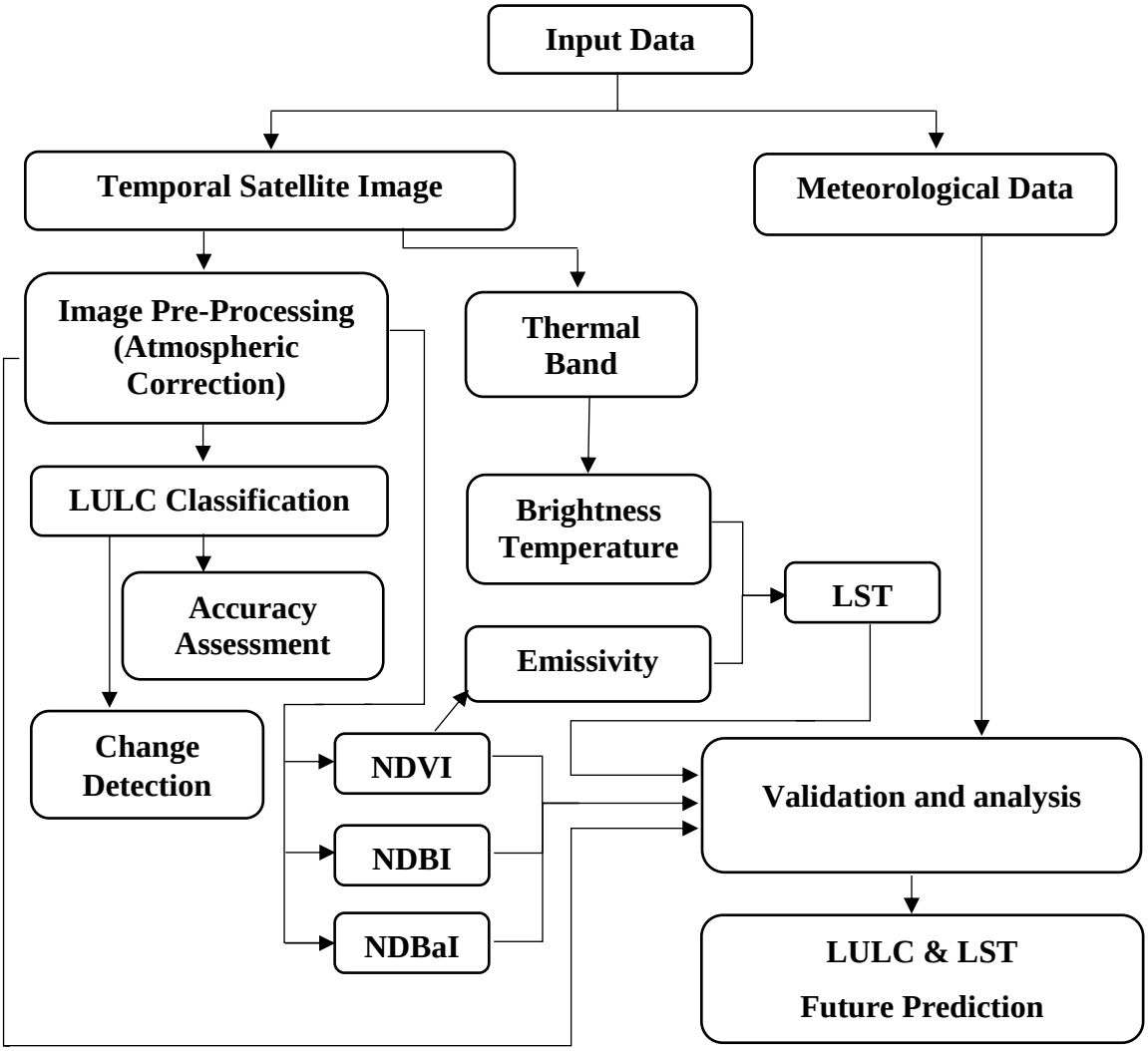

Figure 3.1: Detailed Methodology Flowchart

Table 3.1: Details of the datasets used

Type of Dataset Used	Year	Scale/Resolution
Temperature and Precipitation Data	1992-2017	
Landsat 5 TM Image	1992,1996,2000,2008	30 m
Landsat 8 OLI/TIRS	2014, 2017	30 m
Administrative Boundary Map		1:25, 000

3.2.1 Image Processing

Some image pre-processing techniques such as dark object subtraction method was applied on the images to minimize the land surface and atmospheric effects. After pre-processing the images were cropped according to required study area boundaries using the shapefile of the study area. The condition of null data was applied on the respective satellite imageries so that unavailable area with no digital value could not affect the results during processing and application of formulas.

3.2.2 LULC Classification

Image classification converts spectral raster data into a fixed set of classes that corresponds to different surface types present in the imagery. In order to examine the impact of human activities in the study area, LULC classification is necessary for detection of changes that have been brought up during the urbanization process since 1990s. Supervised classification was done by using maximum likelihood method. A general LULC classification scheme was adopted pertinent to the requirement of research. Four general LULC classes were classified, namely; Built-up, Vegetation, Bare Land and Water. Training sites for specific class types were selected through local knowledge, visual interpretation and in depth analysis of the spectral characteristics.

3.2.3 Brightness Temperature

Brightness Temperature (BT) is basically the black body temperature, which is a measure of the photons received by the respective sensor's wavelength presented in units of temperature. Given that the photons are also emitted by water vapors present in atmosphere apart from those emitted by the underlying surface, it is therefore the combination of both (Visible Earth 2008). BT can be derived from the radiances computed from thermal infrared sensors at the top of the atmosphere by using Plank's

law, which describes the spectral radiance of electromagnetic radiation at all wavelengths from a black body at a certain temperature (Dash *et al.,* 2002).

3.2.3.1 Computation of brightness temperature

Brightness Temperature was derived in two phases, as proposed by Chen *et al.* (2002). In the first phase, the Digital Number (DN) of the thermal band, i.e. band 6 and band 10 for Landsat 5 and Landsat 8 respectively, are converted into radiance luminance (R_{TM}) as shown in Equation 3.1. In the second phase, this derived ration luminance is converted to at-satellite brightness temperature in kelvin through equation 3.2.

$$R_{TM} = B_{TIR} / 255 \, (R_{max} - R_{min}) + R_{min} \qquad (3.1)$$

Where

B_{TIR} = DN value of Thermal band

R_{max}, R_{min} = Constants (the values of these constant are given image metadata (MTL.txt) file

R_{TM} = Radiance Luminance

$$BT = K_1 / Ln(K_2 / R_{TM}) / B_{TIR}) + 1 \qquad (3.2)$$

Where,

K_1 and K_2 = Pre-launch calibration constants (also found in metadata file)

3.2.4 Derivation of Indices

For the evaluation of LST, in association with the major land cover types three basic indices, namely; Normalized Difference Vegetation Index (NDVI), and Normalized Difference Bareness Index (NDBaI), and Normalized Difference Built-up Index (NDBI) were used(As-syakur *et al.*, 2012; Karnieli *et al.*, 2010). As their names indicate, these indices target the three major land cover types, i.e. vegetation, bare land and built-up area respectively. Since the given indices for Landsat 5 have been extensively used in literature, they can therefore be used as a correct source of derivation of same indices for other satellites. The indices are based on simple band rationing, making use of specific wavelength ranges which enhance the spectral characteristics of the image and bring forward the required features like vegetation, water content etc. The methodology applied for current study is reliable as it is simply the comparison and then selection of the same wavelength ranges for Landsat 8 as previously used for Landsat 5 respectively. The details are given below:

3.2.4.1 Computation of NDVI

NDVI is the most widely used vegetation index developed by Purevdorj *et al.*, (1998). It estimates the presence, vigor and density of vegetation in an area through band ratioing of red and near infrared wavelengths. The value ranges between -1 to +1, with positive values indicating vegetated areas and negative values indicating non-vegetated surfaces. The NDVI equations used for Landsat 5 and Landsat 8 are given below respectively.

$$NDVI = \frac{(Band\ 4 - Band\ 3)}{(Band\ 4 + Band\ 3)} \qquad (3.4)$$

$$NDVI = \frac{(Band\ 5 - Band\ 4)}{(Band\ 5 + Band\ 4)} \qquad (3.5)$$

3.2.4.2 Computation of NDBI

NDBI (Zha *et al.,* 2003) was used for extracting the built-up area from the image. Equation 3.6 and 3.7 expresses this index for Landsat 5 and Landsat 8 respectively.

$$NDBI = \frac{(Band\ 5 - Band\ 4)}{(Band\ 5 + Band\ 4)} \qquad (3.6)$$

$$NDBI = \frac{(Band\ 6 - Band\ 5)}{(Band\ 6 + Band\ 5)} \qquad (3.7)$$

3.2.4.3 Computation of NDBaI

For retrieval of bare land from the image, NDBaI (Zhao & Chen, 2005) was used. This index clearly differentiate the bare land pixels from those of built-up, as both these LC types have almost same spectral characteristics. The equation 3.8 and 3.9 were used for Landsat 5 and Landsat 8 respectively.

$$NDBaI = \frac{(Band\ 5 - Band\ 6)}{(Band\ 5 + Band\ 6)} \qquad (3.8)$$

$$NDBaI = \frac{(Band\ 6 - Band\ 10)}{(Band\ 6 + Band\ 10)} \qquad (3.9)$$

3.2.5 Retrieval of Land Surface Temperature (LST)

Since the brightness temperature gives the temperature of both; atmosphere and surface, it wasn't sufficient in accurately relating the UHI and LULC type changes in the study area. Hence it was essential to derive the LST in order to evaluate the precise relationship. For this purpose, the retrieval of emissivity was essential, which was accomplished by adopting the method given by Bastiaanssen *et al* (1998). This method uses the values of NDVI as a source for calculating emissivity of an image (equation 3.10). The relation is only valid for NDVI values greater than 0.16. Therefore, an adjustment (based on

literature) was made for NDVI less than 0.16. NDVI less than 0.16 (positive) is normally bare land and semi bare land. Therefore for this value the emissivity was set to 0.92 and for NDVI less than 0 (normally built-up and water surfaces) the emissivity was set to 1 (Gieske and Timmerman, 2002).

$$\varepsilon_o = 1.009 + 0.047.\ \text{Ln (NDVI)} \qquad (3.10)$$

After the calculation of emissivity, the final step for the retrieval of land surface temperature was accomplished by taking into account the brightness temperature and emissivity using equation 3.11, as given by Landsat Project Science office (2002).

$$\text{LST} = \frac{\text{BT}}{\varepsilon_o{}^{0.25}} \qquad (3.11)$$

3.2.6 GIS Analysis

GIS technology caters for addition, manipulation, organization and analysis of geospatial data, hence providing a platform for almost all disciplines of science to carry out their decision making processes efficiently and diligently. The main events in present GIS analysis of the satellite's remotely sensed data and meteorological data include image analysis and statistical analysis. Relevant literature was consulted to select appropriate analytical techniques for qualitative and quantitative analysis of the data, leading towards the fulfillment and justification of the research hypothesis and objectives.

3.2.6.1 TEMPORAL ANALYSIS OF LULC CHANGES

A general LULC classification scheme was adopted from Anderson *et al.*, (1976). Four classes were determined by taking into account the spatial resolution of the image bands.

The selected classes and their brief description is given in Table 3.2. Basically four classes were assigned to the scenes of Landsat.

Accuracy assessment of all classified images was done through ERDAS Imagine's accuracy assessment tool. The tool enables evaluation of pixels in a classified image to be selected randomly with stratified sampling. This was carried out through visual interpretation, by taking random sampling points across the study area that were relatively uniformly distributed among the LULC types. Once the true identity of all evaluation pixels is specified, the tool automatically generates statistics such as overall accuracy (in percentage) and Kappa statistics (ranging from 0 to 1). Comparison of an actual classification results with a commonly accepted standards depicts the effectiveness of the classification over randomness. The comparison results is measured by the Kappa test statistic (Gao, 2009). The overall accuracy and kappa statistics for each year is given in Table 3.3 which falls in the range of (90-93) % and (0.87- 0.9) respectively which is quite an acceptable rang. The percentage area of each LULC type was calculated from the image based on the number of pixels falling in each class through raster calculator in ArcGIS. Table (3.4 -3.6) show the area in Km^2 and percentage of LULC classification in Lahore for different images. The resultant yearly LULC classified images (1992, 1996, 2000, 2008, 2014 and 2017) are shown in Figure 3.3 and 3.4. The overall LULC changes in study area are discussed in Section 4.1.

Table 3.2: Selected LULC scheme defining each class type according to Anderson et al., (1971 & 1976).

No.	LULC TYPE	Description
1	Built Up	Areas with land covered by impervious materials (concrete, asphalt etc.), including buildings and roads.
2	Vegetation	Mixture of grasslands, parks, green-belts and woodland having tree crown areal density
3	Water	Lakes, reservoirs and streams
4	Bare Land	Mixture of non-vegetated land, cropland with stubble remaining, transitional areas where any type of land use ceases as areas become temporarily bare as construction is being planned

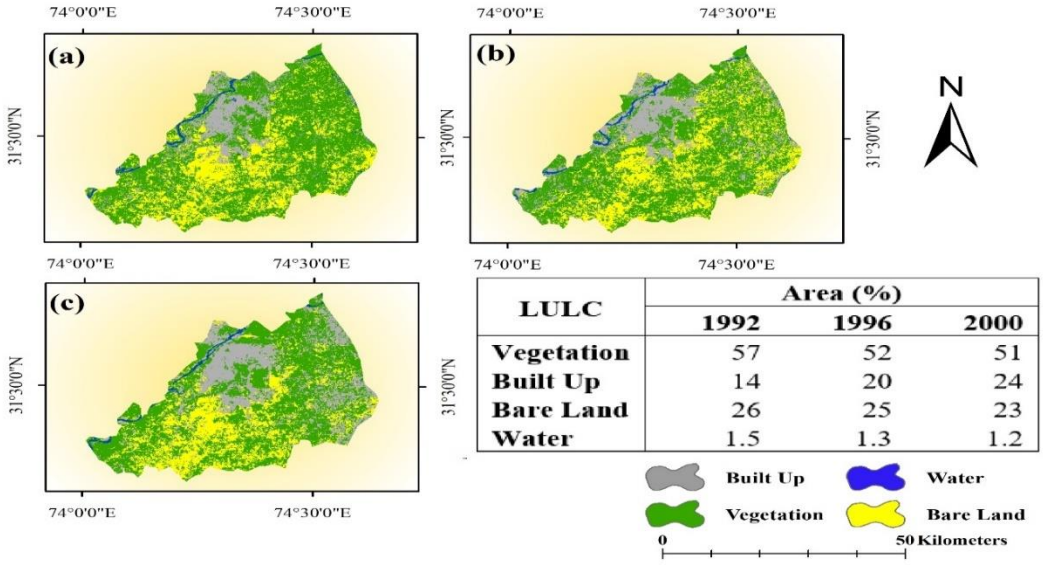

Figure 3.2: LULC maps of study area dated (a) 9th June 1992 (b) 4th June 1996 (c) 30th May 2000.

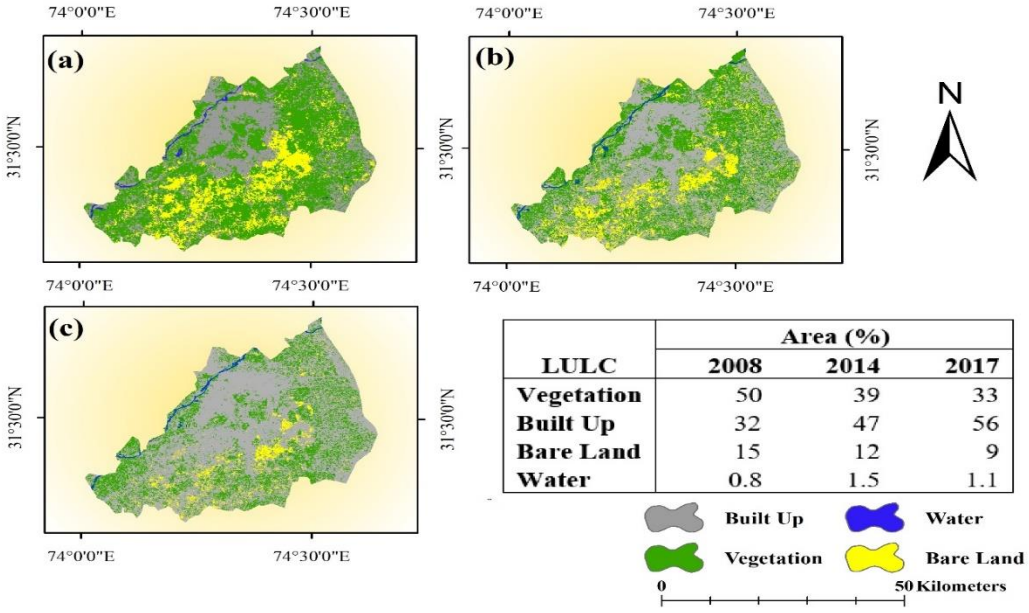

Figure 3.3: LULC maps of study area dated (a) 5th June 2008 (b) 6th June 2014 (c) 14th June 2017.

Table 3.3: Overall accuracy and kappa statistics of LULC Classification

Year	Overall Classification Accuracy	Overall Kappa Statistics
1992	90.8	0.87
1996	91.2	0.89
2000	90.7	0.83
2008	90.3	0.9
2014	92.6	0.9
2017	90.3	0.88

Table 3.4: LULC in 1992 and 1996

CLASS NAME	1992		1996	
	Area (Km2)	%age	Area (Km2)	%age
BUILT-UP	260.5	14.7	363.26	20.5
VEGETATION	1010	57	928.5	52.4
BARE-LAND	471.4	26.6	453.6	25.6
WATER	26.6	1.5	24.8	1.4
TOTAL	≈1772	≈100	≈1772	≈100

Table 3.5: LULC in 2000 and 2008

CLASS NAME	2000		2008	
	Area (Km2)	%age	Area (Km2)	%age
BUILT-UP	428.8	24.2	581.2	32.8
VEGETATION	903.7	51	894.9	50.5
BARE-LAND	414.6	23.4	278.2	15.7
WATER	21.3	1.2	15.9	0.9
TOTAL	≈1772	≈100	≈1772	≈100

Table 3.6: LULC in 2014 and 2017

CLASS NAME	2014		2017	
	Area (Km2)	%age	Area (Km2)	%age
BUILT-UP	838.2	47.3	1001.2	56.5
VEGETATION	689.3	38.9	590.01	33.3
BARE-LAND	214.4	12.1	161.3	9.1
WATER	28.4	1.6	19.5	1.1
TOTAL	≈1772	≈100	≈1772	≈100

3.2.6.2 LST AND BUILT-UP LAND

In order to evaluate the surface UHI, image derived LST (Figure 3.5) were used in comparison with built up to investigate its relationship with LST. The relationship also helped in determining the correlation between these two variables and their significance. This was done by considering the built-up class of all the images, and then calculating its respective area and mean LST. The results showed a notable increase in built-up area from 1992 to 2017 (Table 3.7). By plotting the two variables i.e. built-up area and mean LST through linear regression a positive correlation was observed which showed that both are directly proportional to each other (Figure 3.6Figure 3.5). Detailed results are discussed in section 4.2.

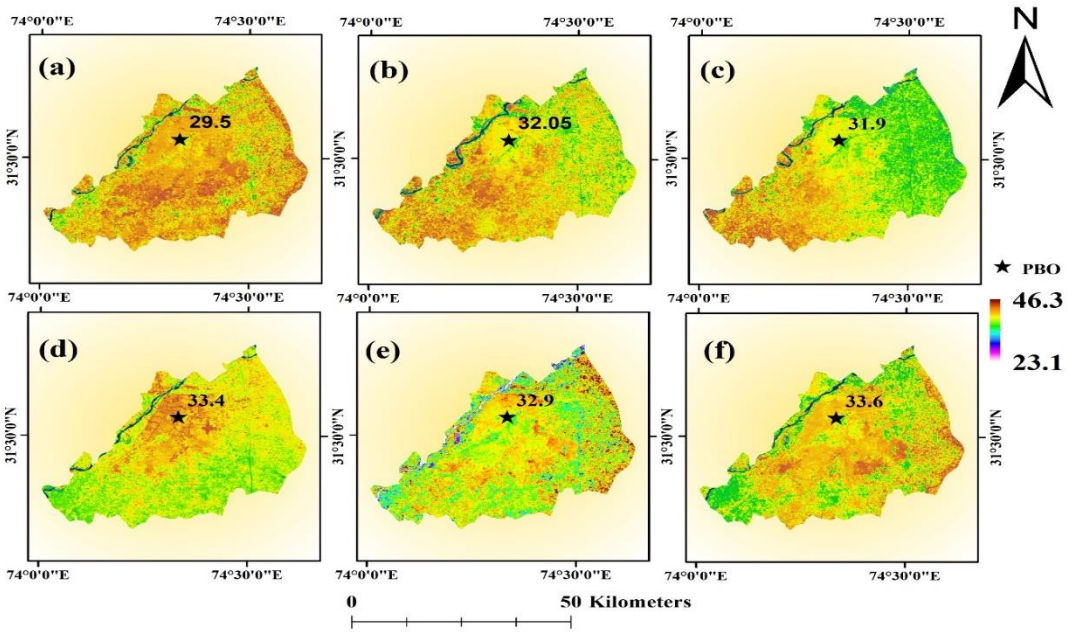

Figure 3.4: LST's Maps of Study area dated (a) 9th June 1992 (b) 4th June 1996 (c) 30th May 2000 (d) 5th June 2008 (e) 6th June 2014 and (f) 14th June 2017.

Table 3.7: Temporal Change in LST and Built up

Year	Area of Built UP (%)	LST
1992	14	29.5
1996	20	32.05
2000	24	31.9
2008	32	33.4
2014	47	32.9
2017	56	33.6

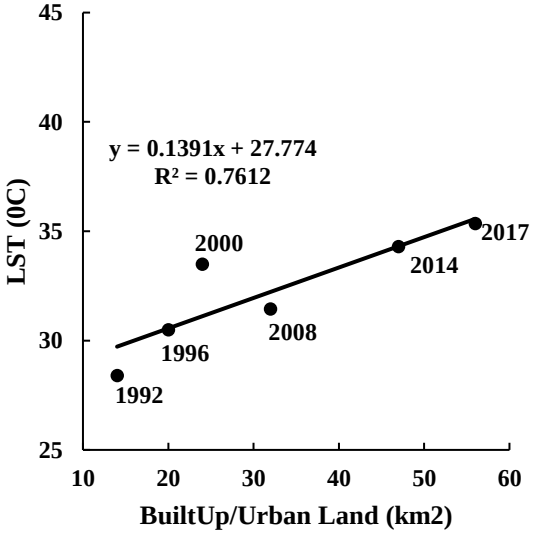

Figure 3.5: Relationship between Built-up and LST

3.2.6.3 LST AND VARIOUS INDICES

The NDVI, NDBI and NDBaI indices were obtained from Landsat 5 and Landsat 8 imageries from 1992-2017. Index value ranges were found to be different for different images due to variation in seasonal, atmospheric and ground conditions of the respective images. Positive NDVI values showed high vegetation cover (0.2 and above) while negative values showed built-up, bare land and water (-1 to -0.01) (Figure 3.7). NDBI values for all the images collectively fell in the range of -0.7 to 0.6, the highest showing built-up and some bare land and lowest showing vegetation and water (Figure 3.8). NDBaI showed the more bare land in June 1992, and the least bare land in June 2017 as shown in Figure 3.9.

The indices were used to efficiently analyze the LULC types as classified from the Landsat 5 and 8 imagery, in order to develop an understanding of the relationship between NDVI, NDBI, and NDBaI and LST by associating the major LULC types. Appropriate threshold values of all the indices were set that helped easily distinguish the classes. The LST was retrieved through the method previously discussed in section (3.2.1). Different temperature ranges resulted from the thermal bands of the images for different classes. Significant changes in temperature were observed during the months of May and June respectively. Details of resultant LST images are presented and discussed in section (4.2).

LULC types were individually extracted from the images through reclassification technique and were categorized into their respective layers. The means of indices for each LULC type (excluding water) were calculated from the respective images through extraction, masking and zonal statistics in ArcGIS. By performing overlap analysis of the LST and classified images for all the four years respectively, the mean LST for overall

generalized LULC classes were estimated as well. Then these mean values of LST, indices and LULC were plotted to quantitatively investigate the relationship between these parameters by using correlation and linear regression analysis, the scatterplots of which are shown and discussed in section (4.3) accordingly.

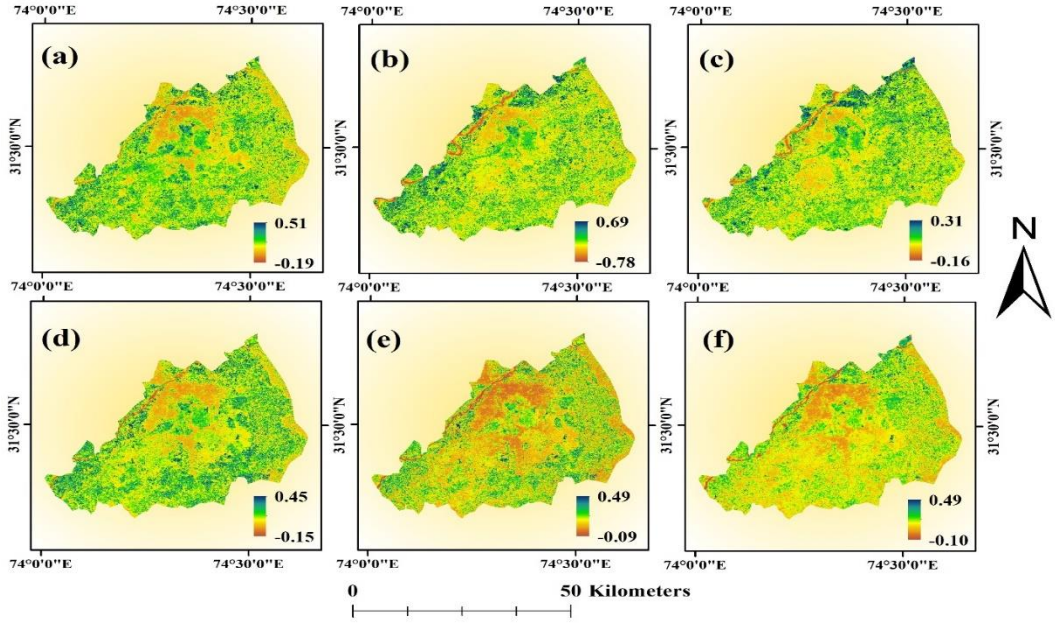

Figure 3.6: NDVI maps of Study area dated (a) 9th June 1992 (b) 4th June 1996 (c) 30th May 2000 (d) 5th June 2008 (e) 6th June 2014 and (f) 14th June 2017.

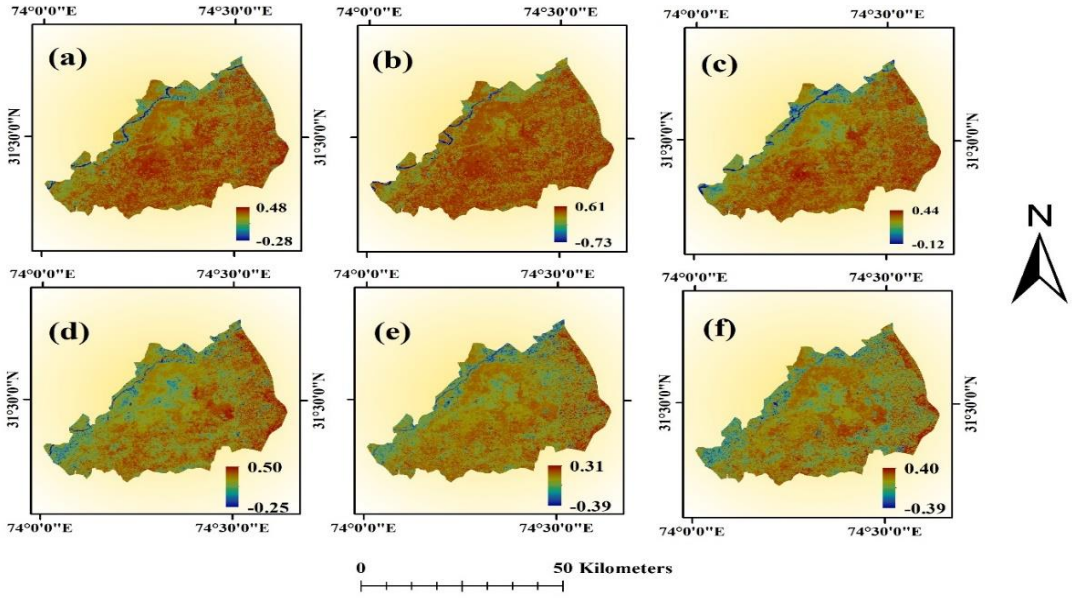

Figure 3.7: NDBI maps of Study area dated (a) 9th June 1992 (b) 4th June 1996 (c) 30th May 2000 (d) 5th June 2008 (e) 6th June 2014 and (f) 14th June 2017.

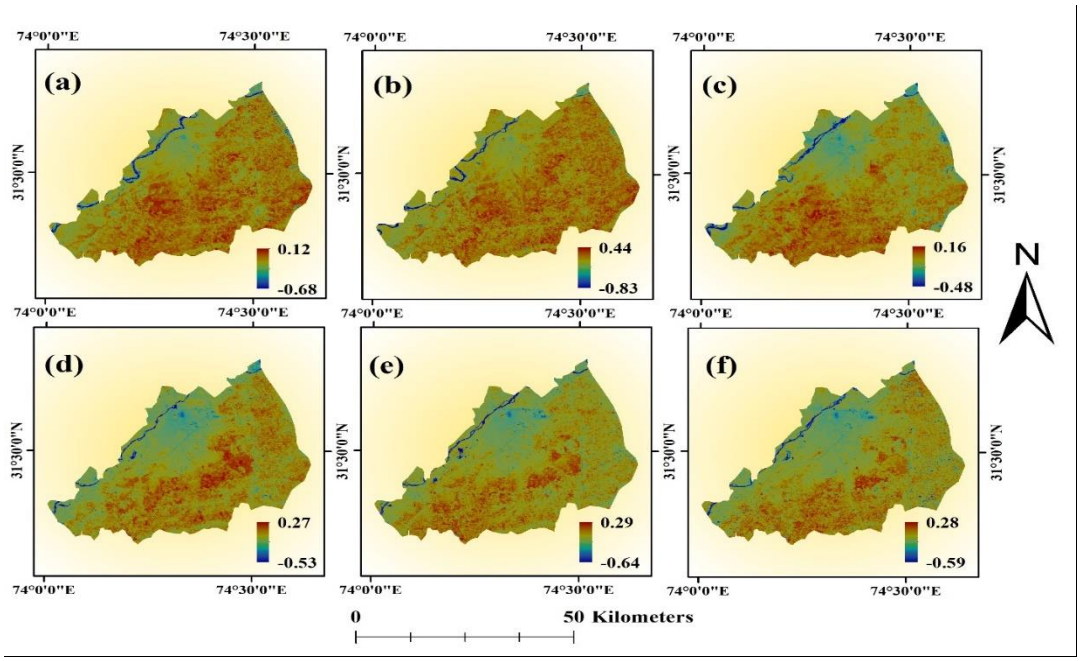

Figure 3.8: NDBaI maps of Study area dated (a) 9th June 1992 (b) 4th June 1996 (c) 30th May 2000 (d) 5th June 2008 (e) 6th June 2014 and (f) 14th June 2017.

Chapter 4

RESULTS AND DISCUSSION

4.1 LULC CHANGES

During the span of 1992-2017, Lahore has experienced drastic changes in the spatiotemporal LULC patterns. Major developments took place in city center where haphazard settlements gave rise to more contiguous pattern of built-up area. Figure 4.1 shows the generalized changes in LULC types in Lahore from 1992 to 2017.

Through percentage wise LULC change analysis, built up area was found to be the most rapidly growing i.e. increasing from 14.7 in 1992 to 56.5 in 2017. As the built up area increased the percentage of bare land decreased from 26.6 in 1992 to 9.1 in 2017. Similarly the vegetation cover also experienced a decline in area from 57 in 1992 to 33.3 in 2017 with a major decrease occurring during the period from 2008 to 2017 (Figure 4.1-4.2). A look at the total percentage difference between the LULC types from 1992 to 2017 clearly shows how a 23% and 17% decrease in Vegetation and bare land respectively resulted in a 41% increase in built up land in 2017 (Table 4.1). The difference is positive when the area of an LULC increased and negative when the area has decreased. It can be seen that all the LULC types had experienced a decrease while built-up had experienced an increase which is almost equal to the sum of the decrease in other LULCs.

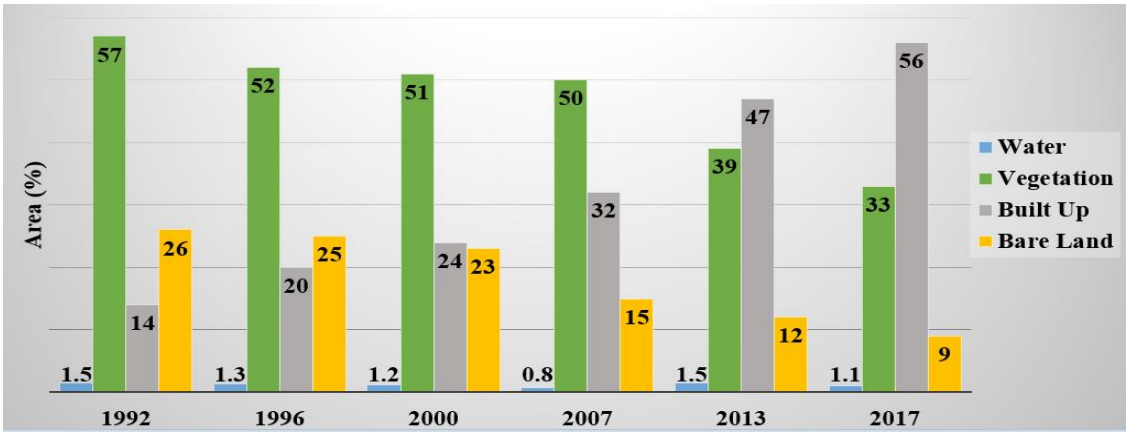

Figure 4.1: LULC Change (1992-2017)

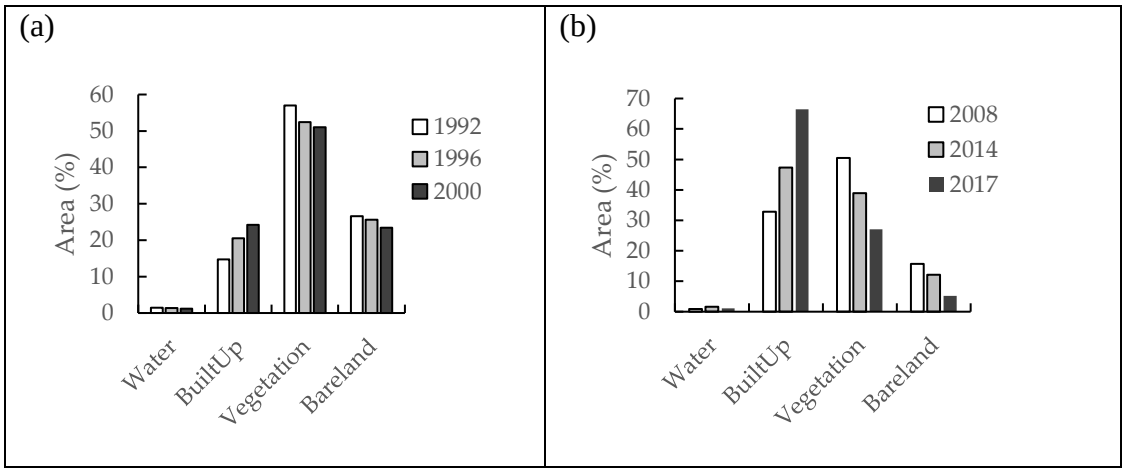

Figure 4.2: LULC Change (a) 1992-2000 (b) 2008 – 2017

Table 4.1: Overall percentage of differences between LULC types in study area

LULC Types	Water	Built-Up	Vegetation	Bare land
1992	1.5	14.7	57	26.6
1996	1.4	20.5	52.4	25.6
Difference	**-0.1**	**5.8**	**-4.6**	**-1**
2000	1.2	24.2	51	23.4
2008	0.9	32.8	50.5	15.7
Difference	**-0.3**	**8.6**	**-0.5**	**-7.7**
2014	1.6	47.3	38.9	12.1
2017	1.1	56.5	33.3	9.1
Difference	**-0.5**	**9.2**	**-5.6**	**3**
Total Difference	**-0.4**	**41.8**	**-23.7**	**-17.5**

4.2 SPATIAL DISTRIBUTION OF LST OVER LULC

The temporal and spatial distribution of LST retrieved from Landsat 5 and Landsat 8 imagery has been shown in section 3.2.6.2 (Figure 3.5). Ambient air temperature data was obtained from weather station falling within the study area. The air temperature for the specific time of image acquisition was used in order to compare it with LST retrieved through image analysis. The comparison showed the variation in temperature near the surface and in the air, depicting the intensity of surface UHIs during day time.

Table 4.2 shows these differences as positive when surface temperature is more and as negative when it is higher than the ambient air temperature. Negative values are observed in 2008 imagery because of more moisture content as a result of precipitation on that particular day. Moreover the difference between LST obtained from image and Weather station data lies within a range of 2 degrees which; as suggested by literature; is quite an acceptable range.

Unlike the increasing trend of LST in all other images 2008 image showed a decrease in temperature. On that particular date the temperature considerably dropped (~35 °C) due to a precipitation of 3.5 mm per hour and the resultant image clearly showed a decrease in LST of natural land cover areas (< 23.1) due to moisture and evapotranspiration as compared to high impervious built up area(>31.45) as illustrated in Figure 3.5d. LST was observed to be highest in June 2017, with temperatures soaring up to approximately 46 °C (Figure 3.5f).

Though an increasing trend is witnessed in the built up areas during the study time period but much disparity is seen in the resulting LST of this class. Apparently the LST of built up areas in May 2000 is more than that of June 2008 (Table 4.3). This can be due to

seasonal variations and the resulting weather conditions in the region during the selected months. On 5th of June 2008 the temperature was found to be relatively lower due to precipitation in study area which resulted in lowering of temperature. The image dated 14th June 2017 showed the highest temperature thus depicting an early start of the peak summer season as compared to previous years as the temperature range that is observed in mid-June 2017 can be observed in late June or Early July in the past. This result shows the effect of radical LULC changes which have amplified the UHI effect, the fact that UHI seems to be influenced by multiple LULC factors apart from built up area size (although being the most important one), such as vegetation density, moisture content and vegetation cover etc.

4.3 Relating LST and Various Indices

The land surface or near land surface temperature can be affected by the nature of land surface cover, ranging from the bare land to built-up areas to vegetation cover types (zhang et al., 2009). This relationship between the land cover and the resulting temperature was quantitatively analyzed for the present study through statistical analysis, as discussed previously in section (3.2.6.2-3.2.6.3). Table 4.4 shows the regression parameters for these relationships.

NDVI can be used as an important measure for vegetation density to evaluate variations in temperature (zhao et al., 2007). Through the association with the LULC types retrieved for the time period of 1992-2017, the results for regression analysis of LST and NDVI showed that a strong negative relationship exist between the two; the scatterplot of which are shown in Figure 4.3. This negative relationship is also being reported by many studies on thermal remote sensing for urban and rural environments (Karnieli *et al.*, 2010; Son *et al.*, 2012; Sun & Kafatos, 2007). Higher mean LST of built up and bare land for 2014 and 2017 resulted in lower mean NDVI values for the same time. Precipitation moisture in

2008 produced an accurate linear negative trend (R^2=0.98), with vegetation cover having the lowest LST and highest NDVI, whereas bare land and built up, with the highest LST and lowest NDVI, respectively. May 2000 showed the lowest $R^{2=}$ 0.74, because of the less variations in the mean NDVI values of these three land cover types.

Scatterplots depicting the relationship between LST NDBI are illustrated in Figure 4.4. Although, the correlation results were substantial for the selected years, but the ambiguity faced by the differentiation of built up land from the bare land through NDBI made the mean NDBI values of the latter more distinct than the former.

The mean values of NDBaI for the corresponding LULC types accurately showed the relationship between bare land and corresponding LST. Figure 4.5 shows the resulting scatterplots for this relationship indicating a statistically significant correlation between the variables (LST, NDBaI, LULC) (R^2= 0.90) for June 2014 and (R^2= 0.89) for June 2017. However, due to presence of moisture in 2008, the LST for bare land dropped considerably while that of built up areas increased thus making the temperature difference between the two higher in accordance with their corresponding NDBaI values. This is demonstrated by a low R^2 of 0.88 (Figure 4.5d)

Table 4.2: Difference between MET station's temperature and image derived LST

Date	MET Station	Surface Temperature °C	Air Temperature (MET Station) °C	RMSE (Landsat-MET Station) °C
09/06/1992		28.4	29.5	1.1
04/06/1996		30.5	32.05	1.55
30/05/2000	**LAHORE**	33.5	31.9	-1.6
05/06/2008	**PBO**	31.45	33.4	1.95
06/06/2014		34.3	32.9	-1.4
14/06/2017		35.35	33.6	-1.75

Table 4.3: Mean LST of LULC types from 1992 to 2017

LULC Type	Mean LST (°C)					
	1992	**1996**	**2000**	**2008**	**2014**	**2017**
Built Up	28.4	30.5	33.5	31.45	34.3	35.35
Vegetation	25.9	29.1	26.2	31.2	29.3	30.7
Bare Land	34.5	35.7	32.6	33.1	36.8	37.2
Water	24.9	25.3	23.5	26.8	27.1	27.5

Table 4.4: Regression parameters for the linear relationship between LST and respective Indices according to their respective regression analysis (* Regression coefficient).

Year		1992	1996	2000	2008	2014	2017
NDVI-LST	***R^2**	0.7966	0.8047	0.7412	0.9728	0.889	0.8509
NDBI-LST	***R^2**	0.8671	0.9793	0.9216	0.9877	0.9639	0.9354
NDBaI-LST	***R^2**	0.8977	0.9333	0.9012	0.8849	0.9076	0.89

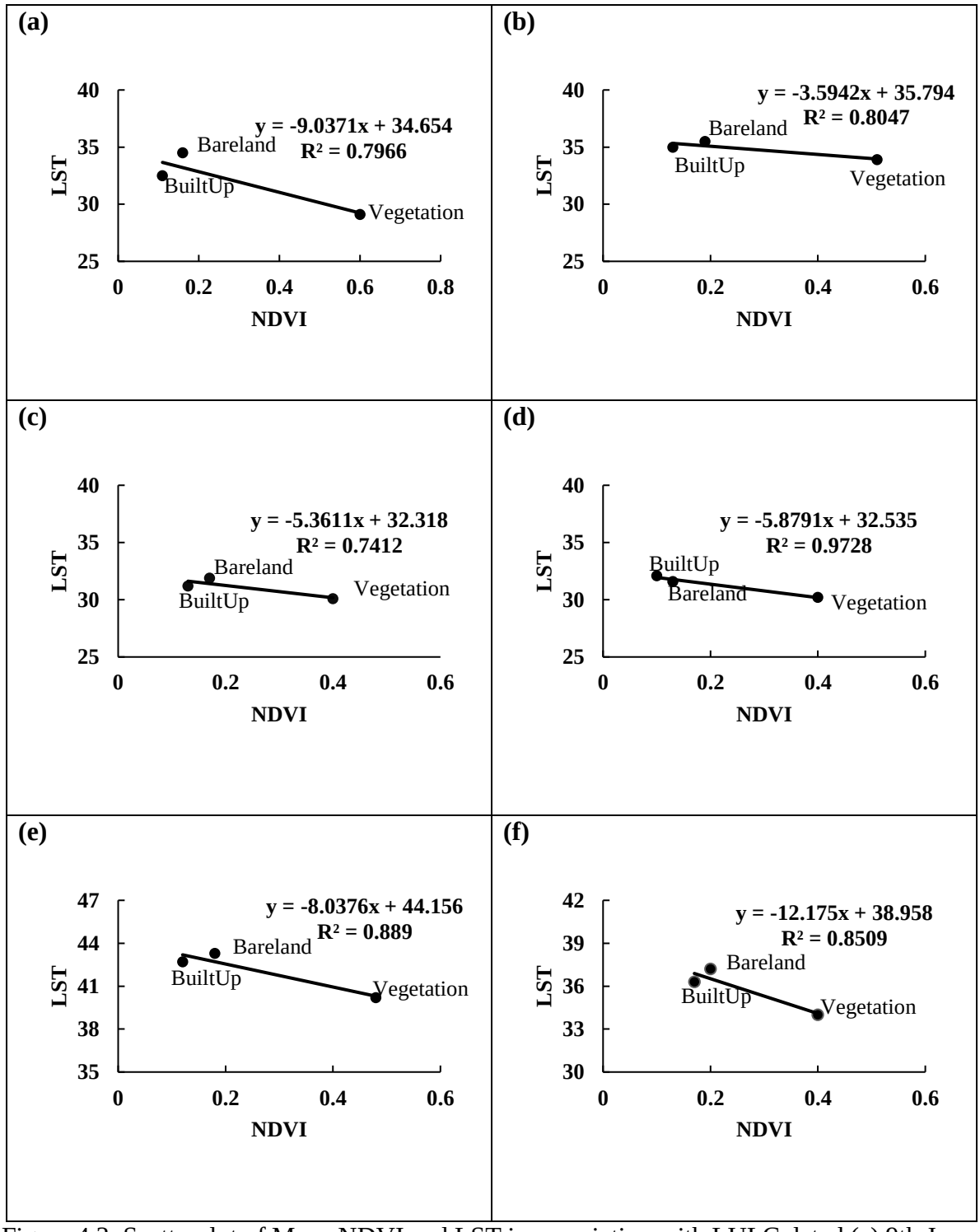

Figure 4.3: Scatterplot of Mean NDVI and LST in association with LULC dated (a) 9th June 1992 (b) 4th June 1996 (c) 30th May 2000 (d) 5th June 2008 (e) 6th June 2014 and (f) 14th June 2017.

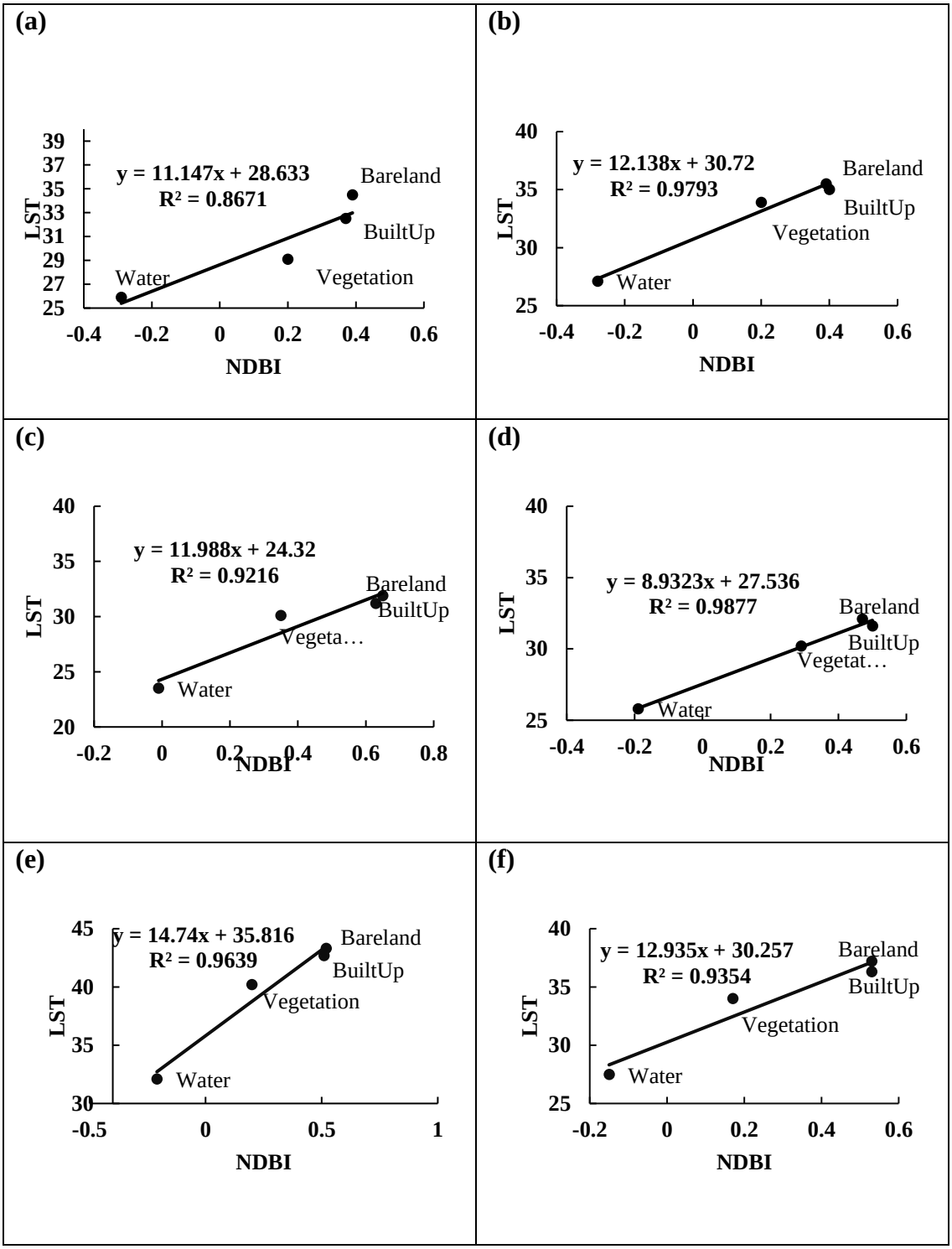

Figure 4.4: Scatterplot of Mean NDBI and LST in association with LULC dated (a) 9th June 1992 (b) 4th June 1996 (c) 30th May 2000 (d) 5th June 2008 (e) 6th June 2014 and (f) 14th June 2017.

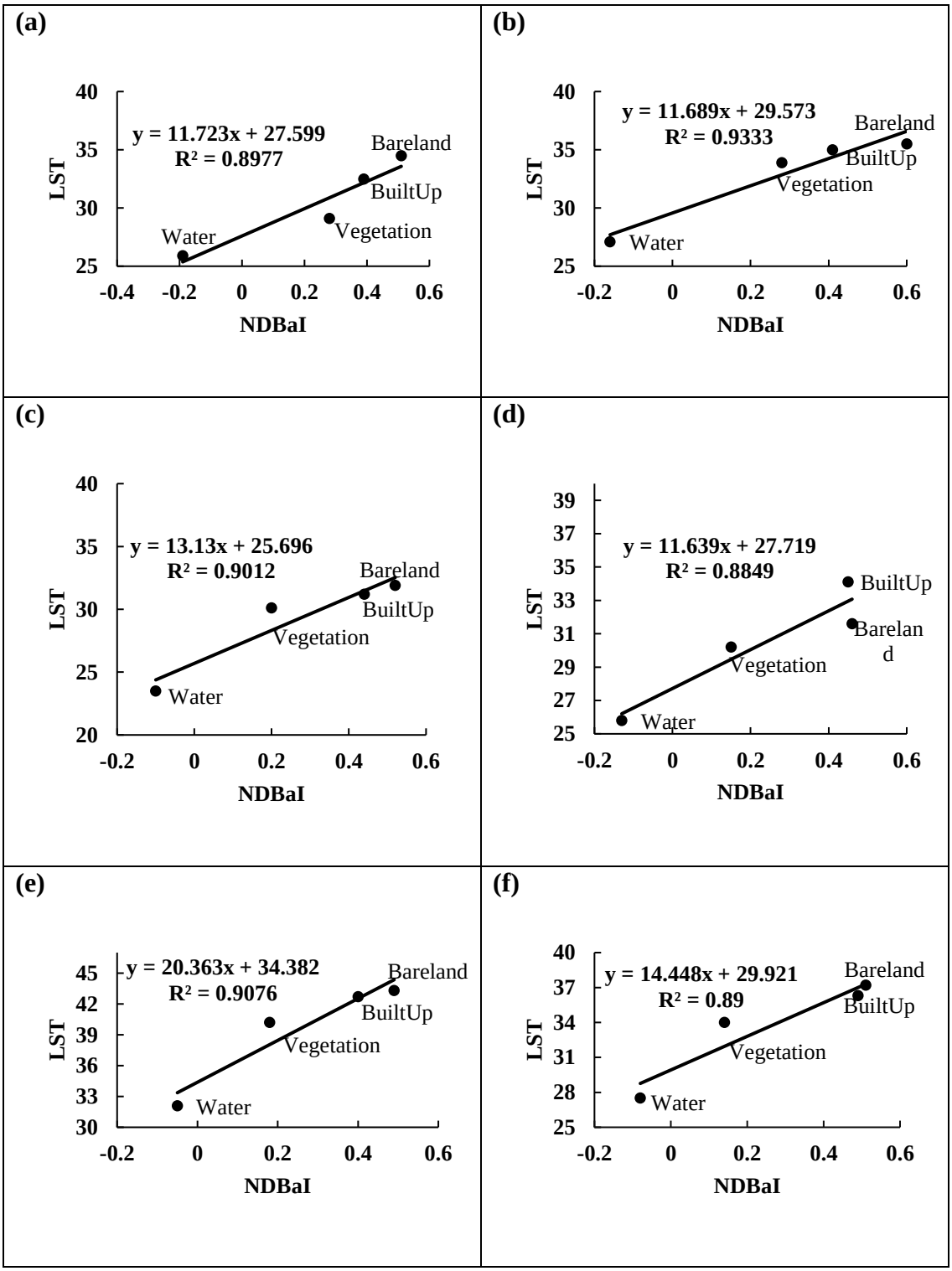

Figure 4.5: Scatterplot of Mean NDBaI and LST in association with LULC dated (a) 9th June 1992 (b) 4th June 1996 (c) 30th May 2000 (d) 5th June 2008 (e) 6th June 2014 and (f) 14th June 2017.

4.4 Relating UHI and LULC Pattern

By extracting the main urban area of Lahore city and analyzing the differences in LST, a great disparity was observed between LST of an urban and a non-urban area. By using a boundary around the urban area/ built up land with reference to 2017 image increase in urban area was also temporally mapped from 1992 to 2017. It was seen that most of the UHIs were formed within the urban area and as the urban extent expanded with the passage of time so does the UHI (Figure 4.6).

4.5 Retrieval, Prediction and Validation of LULC and LST Trend

LST and LULC were predicted by using the existing trend retrieved from the satellite images. Firstly, these values were predicted for the year 2017 and validated by comparing with the actual image derived values. It is worth noting that the difference between actual and predicted LULC values in 2017 remained within the range of 5%, 3%, 1% for built up, vegetation and other LULC respectively (Table 4.5) whereas Difference for LST remained within the range of 1^{o}C (Table 4.6). The High positive value of R2=0.98 for LULC in 2017 (Figure 4.8a) and R^2=0.98 for LST in 2017 (Figure 4.8b) further validated the results. Moreover the temperature predictions for LST suggest that mean temperature is continuously increasing and likely to reach up to 29.01, 32.8, 35.5, and 37.4 in 2030 for Water, vegetation, built up and bare land respectively. Although, the temperature of bare land looks highest but since the area of bare land is continuously decreasing therefore it will cause less contribution in the increase in local and global temperature. The detailed change in LULC and LST and future trend of these variables is given in Table 4.5 & Table 4.6 and expressed in Figure 4.7 respectively.

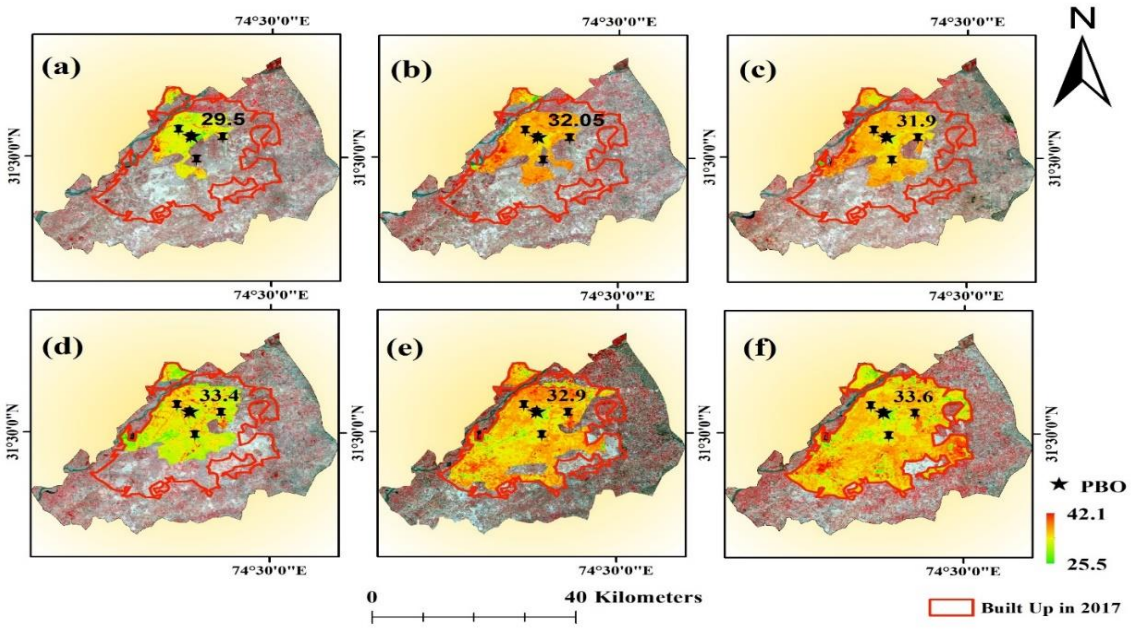

Figure 4.6:Expansion in Built Up Area and Extent of UHI (a) 9th June 1992 (b) 4th June 1996 (c) 30th May 2000 (d) 5th June 2008 (e) 6th June 2014 and (f) 14th June 2017.

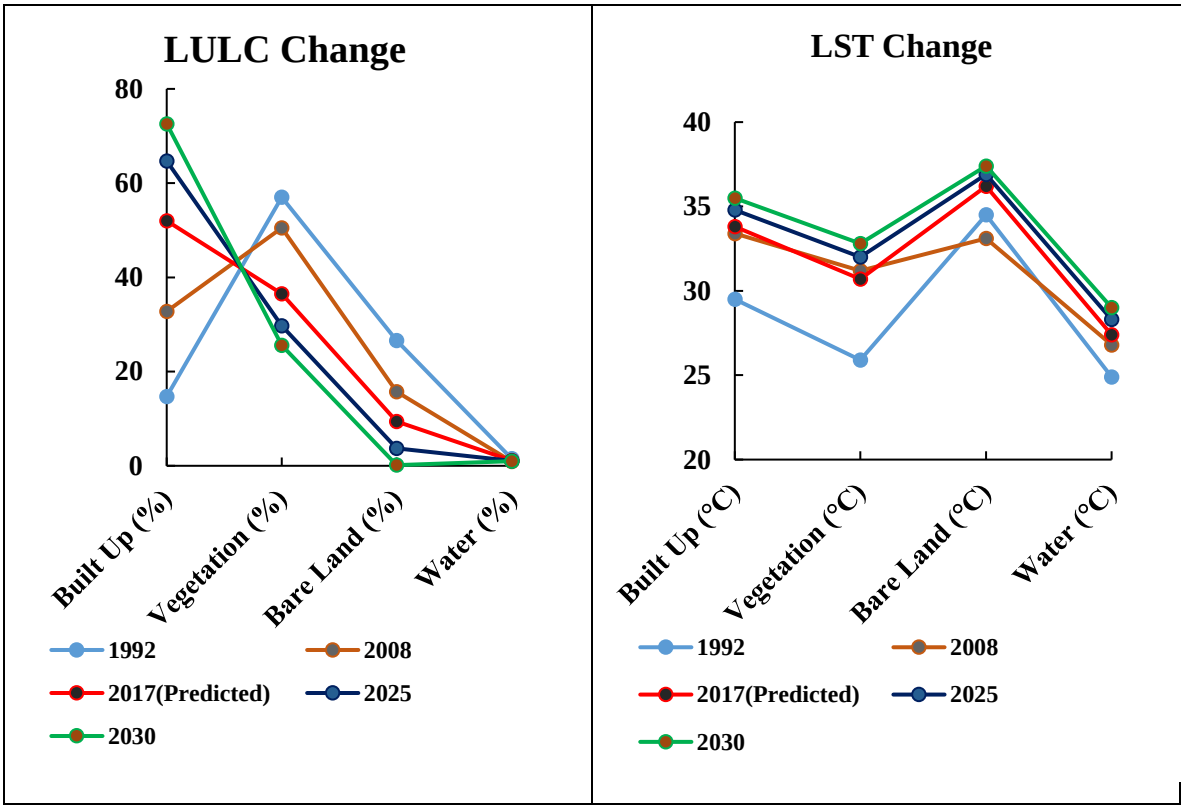

Figure 4.7: LULC and LST timer series analysis

Table 4.5: Previous, Current and Future trends of LULC

Year	Built Up (%)	Vegetation (%)	Bare Land (%)	Water (%)
1992	14.7	57	26.6	1.5
1996	20.5	52.4	25.6	1.4
2000	24.2	51	23.4	1.2
2008	32.8	50.5	15.7	0.9
2014	47.3	38.9	12.1	1.6
2017	56.5 (Predicted=52)	33 (Predicted=36.5)	9.2 (Predicted=9.4)	1.1 (Predicted=1.1)
2021	58.4	33.1	6.6	1.09
2025	64.7	29.7	3.7	1.05
2030	72.6	25.6	0.14	1.01

Table 4.6: Previous, Current and Future trends of LST

Year	Built Up (°C)	Vegetation (°C)	Bare Land (°C)	Water (°C)
1992	29.5	25.9	34.5	24.9
1996	32.05	29.1	35.7	25.3
2000	31.9	26.2	32.6	23.5
2008	33.4	31.2	33.1	26.8
2014	32.9	29.3	36.8	27.1
2017	33.6 (Predicted=33.8)	30.7 (Predicted= 30.7)	37.2 (Predicted=36.2)	27.5 (Predicted= 27.4)
2021	34.3	31.4	36.6	27.8
2025	34.8	32	36.9	28.3
2030	35.5	32.8	37.4	29.01

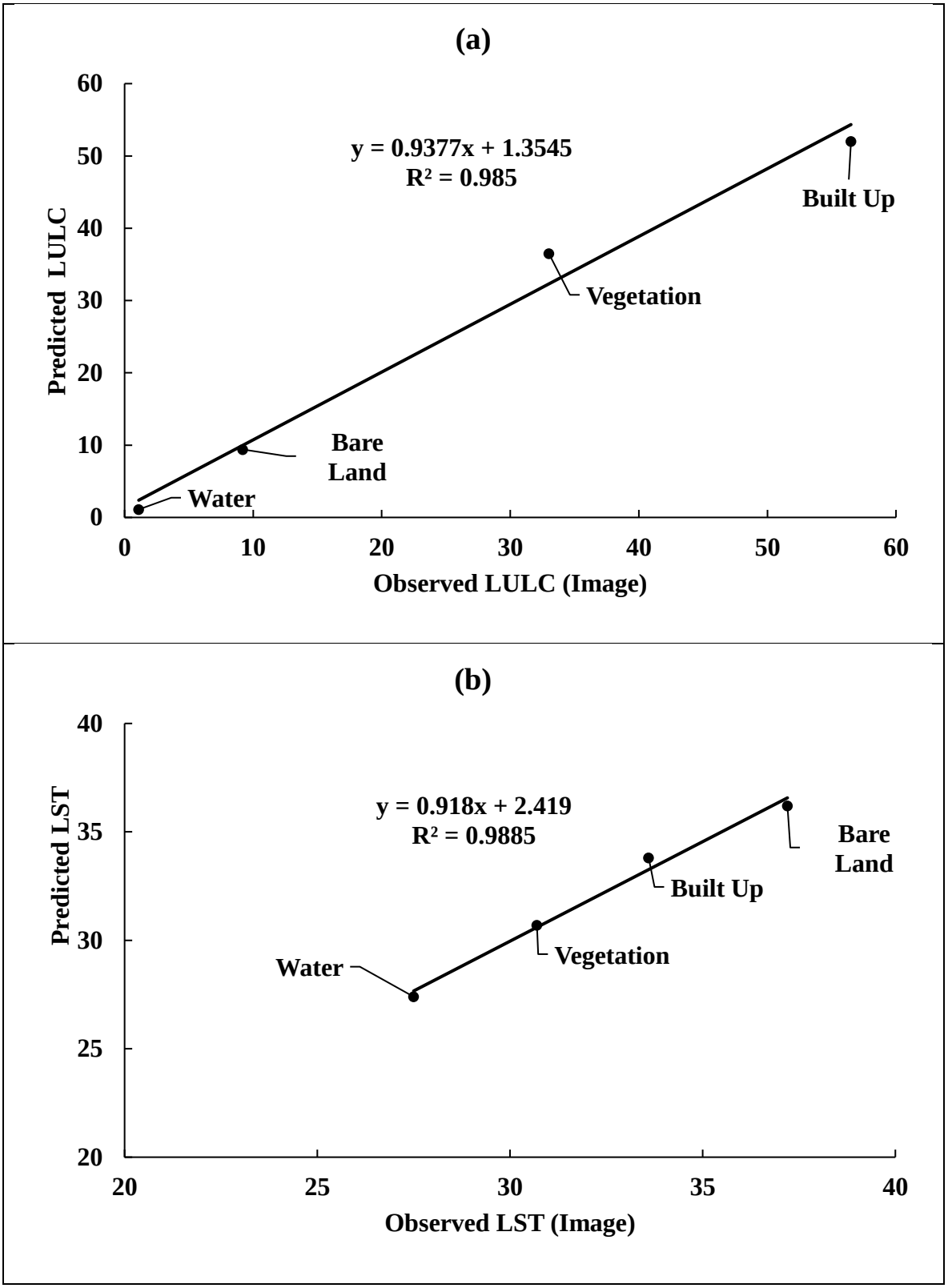

Figure 4.8: Comparison of Image derived and Model Prediction for (a) LULC (b) LST in 2017

Chapter 5

CONCLUSIONS AND RECOMMENDATIONS

This chapter wraps up the research by presenting the findings, along with the recommendations for mitigation of UHI and its future aspects. The study has examined the relationship between surface UHI effect and LULC changes in Lahore, Pakistan, by determining the LST for the period of 1992-2017. All the analysis in this study were based on the interpretation of remote sensing data, suggesting that it can be effectively utilized for analyzing UHI effects.

5.1 Conclusions

Combined analysis of temperature images and LULC maps indicated an evident development of UHI from 1992-2017, depicting significant coherence between the urban thermal patterns and urban spatial distribution. Results indicate that built up area increased by 41% while vegetation cover, bare land and water declined by 24%, 17% and 0.4% respectively. The variations in LST, which determines urban surface thermal spatial patterns and intensities, was found to be affected fundamentally by the spatial distribution and areal extent of different LULC types in the city. Changes in LULC modified the surface reflectance and thus affected the heat and moisture fluctuations. Quantitative analysis and comparison between LST and indices showed that great differences in temperature exists within LULC types, apart from variations amongst different LULC types. Strong positive correlation between NDBI and NDBaI values with LST showed

the significant contribution of built up and bare land types towards the rise in urban temperature.

The observed changes in LULC were mainly attributed to poor land use planning and inconsistent government policies. By comparing the urban temperature with other land uses it was observed that after bare land built up has the highest temperature but since the bare land has a lot been reduced therefore built up is causing more contribution in temperature rise and UHI.

5.2 Recommendation

This study concludes that the percentage of perviousness to imperviousness and depletion of natural vegetation cover form the basis of fluctuations in surface and near surface temperature, paving way for heat islands. Therefore in order to reduce the UHI effect in the city, policies should be taken into account with a focus on;

a. Increasing 'natural' tree and vegetation cover in and around residential and commercial areas. For example planting deciduous trees that provide shade in the summer and allow sun radiations to heat the house in winter, and
b. Avoiding congested development and creating more open spaces through parks and green belts.
c. Recent suggestion by EPA to focus on creating green roofs (also called 'rooftop gardens' or 'eco roofs') can be a good source of cooling buildings.

References

1. As-syakur, A., Adnyana, I., Arthana, I. W., & Nuarsa, I. W. (2012). Enhanced built-up and bareness index (EBBI) for mapping built-up and bare land in an urban area. *Remote Sensing*, *4*(10), 2957-2970.
2. Barnett, T. P., Adam, J. C., & Lettenmaier, D. P. (2005). Potential impacts of a warming climate on water availability in snow-dominated regions. *Nature*, *438*(7066), 303.
3. Buyantuyev, A., & Wu, J. (2010). Urban heat islands and landscape heterogeneity: linking spatiotemporal variations in surface temperatures to land-cover and socioeconomic patterns. *Landscape ecology*, *25*(1), 17-33.
4. Change, I. C. (2014). Mitigation of climate change. *Contribution of Working Group III to the Fifth Assessment Report of the Intergovernmental Panel on Climate Change*, *1454*.
5. Dousset, B., & Gourmelon, F. (2003). Satellite multi-sensor data analysis of urban surface temperatures and landcover. *ISPRS journal of photogrammetry and remote sensing*, *58*(1-2), 43-54.
6. Feizizadeh, B., & Blaschke, T. (2013). Examining urban heat island relations to land use and air pollution: Multiple endmember spectral mixture analysis for thermal remote sensing. *IEEE Journal of Selected Topics in Applied Earth Observations and Remote Sensing*, *6*(3), 1749-1756.
7. Foley, J. A., DeFries, R., Asner, G. P., Barford, C., Bonan, G., Carpenter, S. R., . . . Gibbs, H. K. (2005). Global consequences of land use. *science*, *309*(5734), 570-574.
8. Fu, P., & Weng, Q. (2016a). Consistent land surface temperature data generation from irregularly spaced Landsat imagery. *Remote sensing of environment*, *184*, 175-187.

9. Fu, P., & Weng, Q. (2016b). A time series analysis of urbanization induced land use and land cover change and its impact on land surface temperature with Landsat imagery. *Remote sensing of environment, 175*, 205-214.
10. Grimmond, S. U. E. (2007). Urbanization and global environmental change: local effects of urban warming. *Geographical Journal, 173*(1), 83-88.
11. Higgins, P. A. (2007). Biodiversity loss under existing land use and climate change: an illustration using northern South America. *Global Ecology and Biogeography, 16*(2), 197-204.
12. Kalnay, E., & Cai, M. (2003). Impact of urbanization and land-use change on climate. *Nature, 423*(6939), 528.
13. Karnieli, A., Agam, N., Pinker, R. T., Anderson, M., Imhoff, M. L., Gutman, G. G., . . . Goldberg, A. (2010). Use of NDVI and land surface temperature for drought assessment: Merits and limitations. *Journal of climate, 23*(3), 618-633.
14. Kikegawa, Y., Genchi, Y., Kondo, H., & Hanaki, K. (2006). Impacts of city-block-scale countermeasures against urban heat-island phenomena upon a building's energy-consumption for air-conditioning. *Applied Energy, 83*(6), 649-668.
15. Li, X., Li, W., Middel, A., Harlan, S., Brazel, A., & Turner Ii, B. (2016). Remote sensing of the surface urban heat island and land architecture in Phoenix, Arizona: Combined effects of land composition and configuration and cadastral–demographic–economic factors. *Remote sensing of environment, 174*, 233-243.
16. Maimaitiyiming, M., Ghulam, A., Tiyip, T., Pla, F., Latorre-Carmona, P., Halik, Ü., . . . Caetano, M. (2014). Effects of green space spatial pattern on land surface temperature:

Implications for sustainable urban planning and climate change adaptation. *ISPRS journal of photogrammetry and remote sensing*, *89*, 59-66.

17. McConnell, R., Moody, P., Osborne, D., Byrne, N., & Walker, D. (2009). Urban Heat Islands and their influence on coastal climates. *Coasts and Ports 2009: In a Dynamic Environment*, 565.
18. Miao, S., Chen, F., Li, Q., & Fan, S. (2011). Impacts of urban processes and urbanization on summer precipitation: A case study of heavy rainfall in Beijing on 1 August 2006. *Journal of Applied Meteorology and Climatology*, *50*(4), 806-825.
19. Mitchell, J. M. (1961). Recent secular changes of global temperature. *Annals of the New York Academy of Sciences*, *95*(1), 235-250.
20. Oke, T. R. (1973). City size and the urban heat island. *Atmospheric Environment (1967)*, *7*(8), 769-779.
21. Patz, J. A., Campbell-Lendrum, D., Holloway, T., & Foley, J. A. (2005). Impact of regional climate change on human health. *Nature*, *438*(7066), 310.
22. Son, N., Chen, C., Chen, C., Chang, L., & Minh, V. Q. (2012). Monitoring agricultural drought in the Lower Mekong Basin using MODIS NDVI and land surface temperature data. *International Journal of Applied Earth Observation and Geoinformation*, *18*, 417-427.
23. Stone Jr, B. (2005). Urban heat and air pollution: An emerging role for planners in the climate change debate. *Journal of the American planning association*, *71*(1), 13-25.
24. Stone Jr, B. (2008). Urban sprawl and air quality in large US cities. *Journal of environmental management*, *86*(4), 688-698.

25. Streets, D. G., Yan, F., Chin, M., Diehl, T., Mahowald, N., Schultz, M., . . . Yu, C. (2009). Anthropogenic and natural contributions to regional trends in aerosol optical depth, 1980–2006. *Journal of Geophysical Research: Atmospheres, 114*(D10).
26. Sun, D., & Kafatos, M. (2007). Note on the NDVI-LST relationship and the use of temperature-related drought indices over North America. *Geophys Res Lett, 34*(24).
27. Tayyebi, A., Shafizadeh-Moghadam, H., & Tayyebi, A. H. (2018). Analyzing long-term spatio-temporal patterns of land surface temperature in response to rapid urbanization in the mega-city of Tehran. *Land Use Policy, 71*, 459-469.
28. Tomlinson, C., Chapman, L., Thornes, J., & Baker, C. (2012). Derivation of Birmingham's summer surface urban heat island from MODIS satellite images. *International Journal of Climatology, 32*(2), 214-224.
29. Torok, S. J., Morris, C. J., Skinner, C., & Plummer, N. (2001). Urban heat island features of southeast Australian towns. *Australian Meteorological Magazine, 50*(1), 1-13.
30. Voogt, J. A., & Oke, T. R. (2003). Thermal remote sensing of urban climates. *Remote sensing of environment, 86*(3), 370-384.
31. Ward, K., Lauf, S., Kleinschmit, B., & Endlicher, W. (2016). Heat waves and urban heat islands in Europe: A review of relevant drivers. *Science of the total environment, 569*, 527-539.
32. Weng, Q. (2009). Thermal infrared remote sensing for urban climate and environmental studies: Methods, applications, and trends. *ISPRS journal of photogrammetry and remote sensing, 64*(4), 335-344.

33. Weng, Q., Firozjaei, M. K., Sedighi, A., Kiavarz, M., & Alavipanah, S. K. (2019). Statistical analysis of surface urban heat island intensity variations: A case study of Babol city, Iran. *GIScience & Remote Sensing*, *56*(4), 576-604.

34. Weng, Q., Fu, P., & Gao, F. (2014). Generating daily land surface temperature at Landsat resolution by fusing Landsat and MODIS data. *Remote sensing of environment*, *145*, 55-67.

35. Weng, Q., Lu, D., & Schubring, J. (2004). Estimation of land surface temperature–vegetation abundance relationship for urban heat island studies. *Remote sensing of environment*, *89*(4), 467-483.

36. Xian, G., & Crane, M. (2006). An analysis of urban thermal characteristics and associated land cover in Tampa Bay and Las Vegas using Landsat satellite data. *Remote sensing of environment*, *104*(2), 147-156.

37. Xiao, H., & Weng, Q. (2007). The impact of land use and land cover changes on land surface temperature in a karst area of China. *Journal of environmental management*, *85*(1), 245-257.

38. Xiong, Y., Huang, S., Chen, F., Ye, H., Wang, C., & Zhu, C. (2012). The impacts of rapid urbanization on the thermal environment: A remote sensing study of Guangzhou, South China. *Remote Sensing*, *4*(7), 2033-2056.

39. Yao, R., Wang, L., Huang, X., Niu, Y., Chen, Y., & Niu, Z. (2018). The influence of different data and method on estimating the surface urban heat island intensity. *Ecological indicators*, *89*, 45-55.

40. Yuan, F., & Bauer, M. E. (2007). Comparison of impervious surface area and normalized difference vegetation index as indicators of surface urban heat island effects in Landsat imagery. *Remote sensing of environment, 106*(3), 375-386.
41. Zhang, Y., Odeh, I. O., & Han, C. (2009). Bi-temporal characterization of land surface temperature in relation to impervious surface area, NDVI and NDBI, using a sub-pixel image analysis. *International Journal of Applied Earth Observation and Geoinformation, 11*(4), 256-264.
42. Zhou, W., Huang, G., & Cadenasso, M. L. (2011). Does spatial configuration matter? Understanding the effects of land cover pattern on land surface temperature in urban landscapes. *Landscape and urban planning, 102*(1), 54-63.